

NON-LINEAR APPROACHES TO THE RESPONSE OF BRICK MASONRY WALL TO LATERAL LOADING

*Miroslav Mynarz¹ and Lucie Mynarzova²

¹Faculty of Safety Engineering, VSB – Technical University of Ostrava, Czech Rep.; ²Faculty of Civil Engineering, VSB – Technical University of Ostrava, Czech Rep.

*Miroslav Mynarz, Received: 11 June 2017, Revised: 27 July 2017, Accepted: 1 Dec. 2017

ABSTRACT: The response of brick masonry wall subjected to lateral loading is presented in this paper. Modelling and analysis of masonry seems to be complicated due to two-component material with different properties and dimensions. Out-of-plane loading adds another issue to be solved. Therefore, it is necessary to perform a calibration to evaluate the dynamic properties of the structure. The response of the finite element model is improved by predicting the parameter by performing a non-linear structural analysis. The deformations obtained numerically were compared to that of experimental observations. The experiments were carried out in one of the experimental galleries in the limestone pit. The study deals with the response of the masonry separating walls at various thicknesses, mechanical properties or loading. This contribution compares the effect of variability of particular parameters to the response of the walls. The results could be used for explosion prevention and protection; masonry buildings are taking into account considering the danger of explosion of natural gas or other items. For favourable design or assessment of masonry wall exposed to the out-of-plane load, which involves also explosion, it is possible to calculate the structure using some finite element model.

Keywords: Brick Masonry, Separating Wall, Explosion, Dynamic Response, Nonlinear response

1. INTRODUCTION

Sorted by their purpose, underground premises involve transportation structures, engineering structures and others (water silo, silo gas, sewerage plant, storage area etc.). Underground galleries interconnecting particular areas are designed with specific aims mainly as transport and airing connections. Purpose and lifetime of underground galleries should be in balance with precautions given on the basis of deep risk analysis. Leakage or formation of flammable gases in such areas certainly represents high risk for interconnected underground locations. Immediate presence of these gases could cause the explosion when open flames or other ignition source occur at the same time.

To prevent propagation and transfer of the explosion, separating or dam walls are built in the galleries. These structures separate two independent areas with no need to pass through or they close unused halls or premises. In the Czech Republic dam or separating walls are usually built from masonry (Fig. 1) however other materials as plaster or fly ash could be also used.

In the case of accidental event, e. g. explosion, these separating structures are subjected to considerable load therefore they should be designed with sufficient resistance. For effective design and assessment of these walls, in-situ experiments should be carried out to provide

useful information about the structures behaviour. Together with the experiments, advanced numerical modelling seems to be another suitable instrument for separating wall design.



Fig. 1 View of the underground gallery

2. EXPERIMENT VENUE

The experiments were carried out [1] in one of the experimental galleries in the limestone pit in Stramberk, Czech Rep. The galleries are used for research and tests in the field of explosion prevention. There are three horizontal parts, two of them are parallel. Concerned gallery measures 300 m (Fig. 2) and its clear section is 10.2 m² in testing part.

Inside the gallery two separating walls were built with the distance of 5.7 m between them. Inside the confined sector, steel frame was embedded in concrete. Loaded structures are placed into this frame with dimensions of 2200 x 2575 mm.

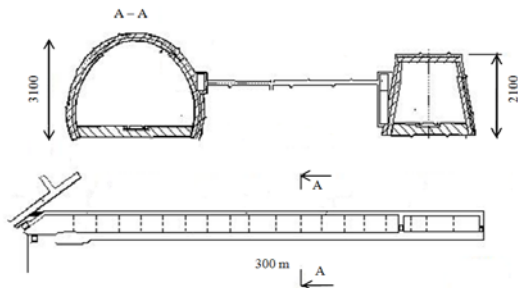


Fig. 2 View of the experimental gallery in Stramberk

There are two pipes with inner diameter of 800 mm at the edge of the barriers. The pipes provide regulation of applied pressure by changing of their free inner diameter. The confined sector and loaded wall are shown in Fig. 3.

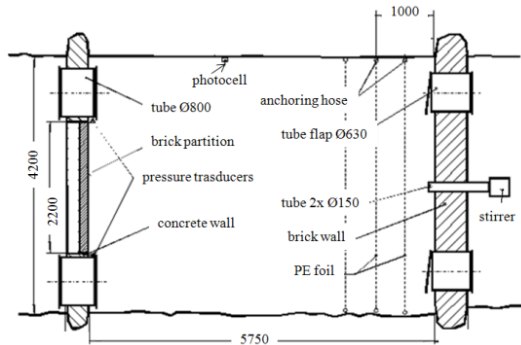


Fig. 3 Confined sector between barriers

The gassed track is located opposite the loaded wall and it is bounded by the dividing barriers and diaphragm of PE sheeting. This sheeting is fixed by rubber hose to the gallery wall. Pressure tank with methane stands out of the sector. Methane is dosing into the confined sector in parallel with stirring the methane-air mixture. Two ways of stirring were suggested: by ejector straight in the confined sector or by ventilator outside the confined sector which should be connected by pipe with diameter of 150 mm. As ejector did not guarantee the homogeneity of the mixture, only ventilator is used for stirring. During filling and stirring the mixture, methane concentration is measured in different height levels using single gas detectors. The way of ignition affects the final explosion parameters. For these experiments, the electrical ignitor with the ignition energy of 80 J

was chosen. The centre of the confined sector, or alternatively the centre of back wall, was chosen as the ignition point. The explosion pressure was recorded by two pressure transducers [2].

2.1 Experimental Parameters

The separating walls of three different thicknesses are dealt with in this paper – 65 mm, 140 mm and 290 mm. This corresponds to the dimensions of used clay bricks (290 x 140 x 65 mm). Their strength is denoted as P10 which corresponds to the compressive strength of the unit 10 MPa; density is considered as $1800 \text{ kg} \cdot \text{m}^{-3}$ and flexural strength is 1.7 MPa. Compressive strength of used cement-lime mortar is between 4 and 5 MPa after 28 days. Used strength characteristics of masonry separating wall result from the standard Eurocode 6 [3]. Other mechanical characteristics of the separating walls are presented in other papers [1], [4]. The dimensions of the walls are approximately 2.2 m width and 2.5 m height, depending on used micromodel or macromodel and particular thickness of the wall.

Each wall was modelled as restrained along all four sides. The load on the structure was considered both as quasi-static action and as real time behaviour measured in the gallery during explosion of methane-air mixture [5]. Corresponding measured load was used for the masonry structure. The explosion pressure is acting like uniform continuous load on the separating wall. For each separating wall of various thicknesses, different values of pressure load were considered according to conducted experiments. Models of the masonry separating walls were created in software ANSYS [6] as it is described later in this paper.

2.2 Numerical Modelling of Masonry

Numerical modelling of masonry brings several issues to be solved. Masonry is a heterogeneous and anisotropic material composed of units (bricks, stones) and mortar. These two components differ in material characteristics, behaviour or dimensions. Disposition of units in masonry in a regular pattern or interface between brick and joint could be taken into account as well. Common software usually offer isotropic materials and necessity of simplified – homogeneous – model.

Masonry walls discussed in this paper were modelled using two different approaches according to [7], micromodelling and macromodelling. Detailed micromodel (Fig. 4) consists of bricks and joints. Dimensions and location of bricks correspond to real parameters of clay units. Layers

of mortar (bed and head joints) are modelled between the bricks. Two layers with different bonds are changed regularly through the height of the modelled wall. This micromodel could be useful for modelling of details, for better understanding of local masonry behaviour or for determination of homogenized properties of masonry. Density, Young's modulus of elasticity, Poisson's ratio, eventually shear modulus and others are defined for each material. Detailed micromodel represents disposition of bricks in the best way on the other hand it is also very computationally demanding. It is suitable mainly for academic use or as the first-choice possibility for subsequent calculations.

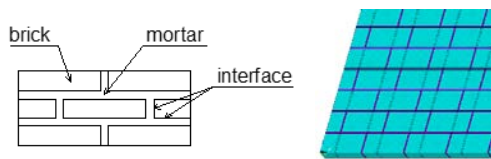


Fig. 4 Detailed micromodel.

In the case of macromodel, neither particular bricks nor mortar layers or their interface are considered. This model is created from one composite (homogenized) material (Fig. 5) which could be isotropic (simplified model) or orthotropic (different strength, stiffness, friction, displacement along the cracks or other parameters could be defined for direction parallel or perpendicular to the bed joints) [8]. The masonry could be homogenized on the basis of constitutive formulas (e. g. modification of models for concrete) or using homogenization techniques (including use of empiric formulas or analysis of detailed macromodel as in [9]). These models are not as precise as macromodel (considering two different materials or units disposition) but they are much less computationally demanding, even for huge structures, and they survey the stress distribution through the whole structure or describe the interaction between particular elements.

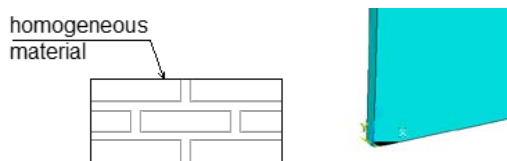


Fig. 5 Homogenized macromodel

2.3 The Classic Drucker-Prager Model

For purpose of this paper, all mentioned walls were modelled both as a micromodel and a

macromodel. Moreover, for non-linear solution two different ways were considered. First approach combines brick element SOLID65 with Drucker-Prager plasticity. The concrete element SOLID65 is used instead of former SOLID45. Orthotropic material properties can be defined if needed. Our homogenized macromodels were created with isotropic characteristics which is simplified version of macromodelling with advantage of easier determination of input data and fast calculation. Classic Drucker-Prager is a rate-independent plasticity model available for frictional material (soil, concrete). It results from Mohr-Coulomb law. Following constants could be used as the input values: the cohesion value c_u

$$c_u = \frac{\sigma_y \cdot \sqrt{3} \cdot (3 - \sin \varphi)}{6 \cdot \cos \varphi} \quad (1)$$

and the angle of internal friction φ

$$\varphi = \sin^{-1} \left(\frac{3 \cdot \sqrt{3} \cdot \beta}{2 + \sqrt{3} \cdot \beta} \right) \quad (2)$$

For known compressive (σ_c) and tensile (σ_t) stresses of material, required constants can be calculated [8] following the material parameter β

$$\beta = \frac{\sigma_c - \sigma_t}{\sqrt{3} \cdot (\sigma_c + \sigma_t)} \quad (3)$$

and stress σ_y

$$\sigma_y = \frac{2 \cdot \sigma_c \cdot \sigma_t}{\sqrt{3} \cdot (\sigma_c + \sigma_t)} \quad (4)$$

Another parameter could be defined: the angle of dilatancy that relates to the amount of dilatancy – the increase in material volume due to yielding. When the dilatancy angle is equal to the friction angle the flow rule is said to be associative. In the case of the dilatancy angle lower than the friction angle (or equal to zero), the flow rule is non-associative and less (or none) volumetric expansion occurs.

2.4 The Concrete Model

For the second, the “concrete model” was studied. This approach of non-linear solution of masonry structures joins the finite element SOLID65 with the concrete material model available also in ANSYS. The eight-node “reinforced-concrete” element SOLID65 is used for three-dimensional modelling of solids. The concrete element SOLID65 is capable of treating the non-linear material properties such as cracking in tension, crushing in compression, plastic deformations or creep features. Reinforcement could be also added. A non-linear elasticity

concrete model could be used for brittle materials (concrete, ceramics), it is suitable mainly for materials with high compressive load-carrying capacity and low tensile strength.

In ANSYS “concrete model”, both crushing and cracking failure modes are included. The concrete model assumes that behaviour is linear elastic until the failure, then crushing or cracking could appear. Three different colours (red, green, blue) are used for the first, second or third cracks [11].

Tension cracks can occur in three different planes of the element and they are illustrated by a circle outline in the plane of the crack, i. e. perpendicular to the direction of the principal stress in one of the integration point of the element. In the case that more than one integration point has cracked, the circle lies in the average direction of all cracked planes of the element. Cracking occurs when the principal tensile stress in any direction lies outside the concrete failure surface that is shown in Fig. 6. Similarly, when all principal stresses are compressive and lie outside the failure surface, crushing occurs.

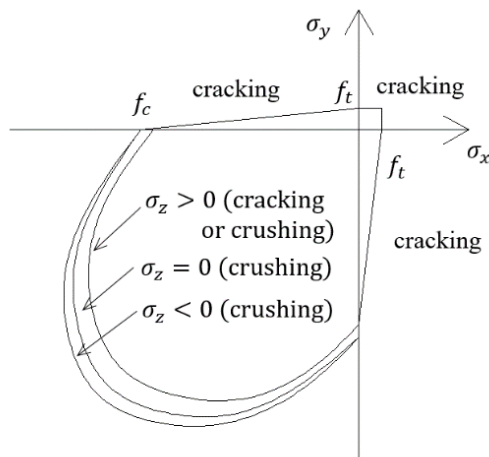


Fig. 6 Concrete failure surface [6]

Behaviour of the model is described, among others, through uniaxial cracking stress, uniaxial or biaxial crushing stress and shear transfer coefficients which take into account sliding across the crack face. Shear transfer coefficient for an open crack β_t varies from 0 to 1. Zero value expresses smooth cracks with complete loss of shear transfer and number 1 represents rough cracks without loss of shear transfer [12]. However, very low values (under 0.1) do not need to lead to convergence. Shear transfer coefficient for a closed crack β_c ranges from 0 to 1 as well. Comparison of cracks in homogenized macromodel is illustrated in Fig. 7. For the illustrative example, both shear transfer

coefficients were chosen as 0.1 (left) or 0.9 (right).

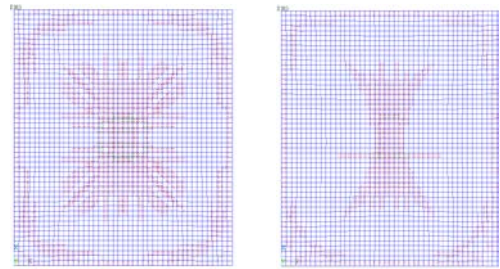


Fig. 7 Illustrative examples of various shear transfer factors

3. RESULTS AND DISCUSSION

3.1 The Concrete Model

Masonry wall under out-of-plane load (earthquake, wind, explosion) is subjected to flexure. The cracks occur and develop depending on supports of the wall. In our case, two-way spanning wall is considered with all four sides restrained and it undergoes biaxial bending. Therefore, resulting crack pattern involves a combination of horizontal, vertical and diagonal crack lines [13].

Display of the cracks when SOLID65 element is used could be highly advantageous. Partly, the overview of general behaviour of the structure is given in relation to the presence of the cracks, and moreover the load when the first indications of cracks occur could be pointed out indeed.

Magnitude of pressure at the time of the first cracks appearance is presented on the wall with thickness of 65 mm. The value of pressure load perpendicular to the wall was 6.7 kPa. The first cracks occurred in the middle of the wall at about 10 % of the load (Fig. 8, left) which corresponds to the pressure of 0.7 kPa. After increase of applied load, cracks progressively spread to the corners of the wall. Later phase of cracks pattern at the pressure of 1.1 kPa is shown in Fig. 8, right. Together with cracks in the middle of the numerical model, gradually developing cracks occur also along the supports.

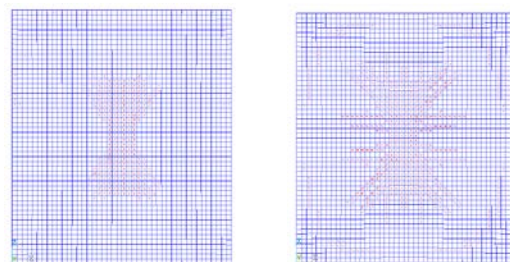


Fig. 8 The first cracks at 10 % (left) and 16 % (right) of applied pressure

Detail of cracks in the middle of the homogenized macromodel is presented in Fig. 9. The first and the second cracks are outlined with particular directions.



Fig. 9 Detail of crack pattern of homogenized macromodel

One of the advantage of the detailed micromodel with separately created bricks and mortar is to monitor only one material. Following detail (Fig. 10) shows cracks arrangement in mortar joints in the middle of the wall.

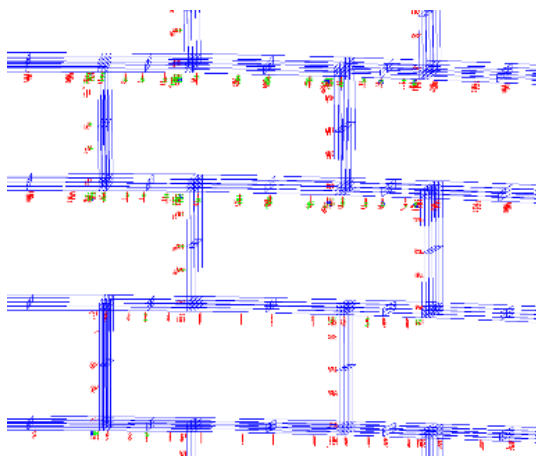


Fig. 10 Detail of crack pattern in mortar joints in micromodel

Following numerical models illustrate deformations of the wall of thickness of 140 mm. Total value of displacement at micromodel (Fig. 11, left) was calculated as 24.8 mm. The other picture (Fig. 11, right) demonstrates deformations at homogenized macromodel with result of c. 25 mm. Both models are in close agreement with each other and the results also correspond to the conducted experiments.

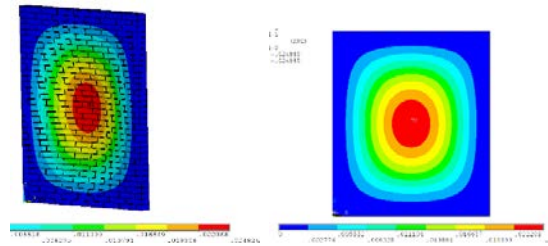


Fig. 11 Total deformations, micromodel (left) and macromodel (right)

3.2 The Classic Drucker-Prager Model

Contrary to the concrete model, Drucker-Prager does not take into account the cracks. Though the calculated deformations are very closed to the measured values. Following figure (Fig. 12) represents the displacements in y direction that was measured as 23.5 mm on the wall with the thickness of 65 mm. Left side shows the micromodel ($u_y = 24.25$ mm) and the macromodel is on the right side micromodel ($u_y = 23.98$ mm).

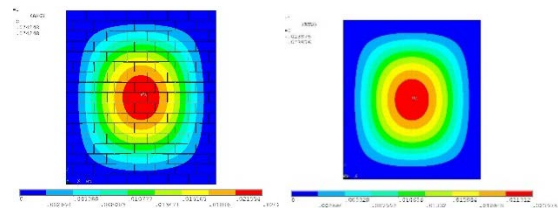


Fig. 12 Deformations in out-of-plane direction, micromodel (left) and macromodel (right)

3.3 Dynamic Load

At real dynamic load, besides dynamic part of the load self-weight is also applied to the masonry separating wall. Such prestress prevents joints and bricks from formation and propagation of cracks. Displacements along the cracks are also limited regarding friction on cracks surface. Ultimate tensile strength, crucial for masonry failure, is – at this type of load – significantly lower compared to compressive strength of masonry. Consequently, the cracks are formed even due to small tensile stresses [14]. The loaded wall is presented on the left side and failure of tested wall is shown on the right side of Fig. 13.



Fig. 13 Masonry wall after explosion [2]

Fig. 14 shows time behaviour of deflection in the middle of the tested partition wall in interaction with the course of explosion load.

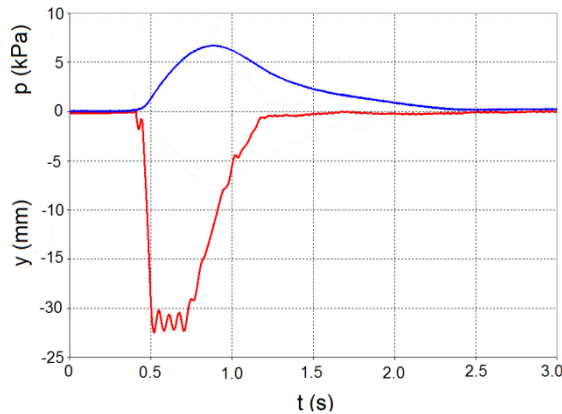


Fig. 14 Measured time behaviour of explosion pressure and deflection during experiment investigation of the wall of thickness 65 mm [15]

3.4 Modal Analysis

At dynamic action lateral to the centre-line of the plated structure of separating wall, this wall behaves like a bending slab. Besides load characteristics, value of dynamic response depends on tune of the structure which is affected by its stiffness and weight. Fig. 15 presents the lowest natural vibration modes of the separating wall. On the left side, the 10th natural mode of homogenized macromodel of the wall of thickness 140 mm is illustrated. 9th natural mode of detailed micromodel of the wall of 290 mm is presented on the right side. Table 1 compares the natural frequencies of the walls created as both micromodel and homogenized macromodel.

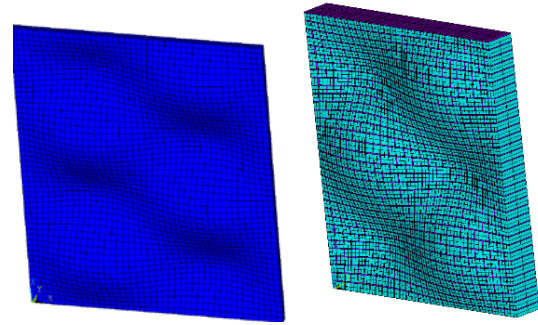


Fig. 15 Natural modes of vibration (left: homogenized macromodel 140 mm, right: micromodel 290 mm)

Tune of the structure is implied in character of the response. If time behaviour of positive phase of the load is significantly longer than the lowest natural vibration frequency, the structure response to the explosion load corresponds to quasi-static deformation of the structure.

Table 1 Calculated natural vibration frequencies $f_{(i)}$ [Hz] of the separating walls

No. of eigenfrequency i	Frequency $f_{(i)}$ for the wall of thickness					
	65 mm		140 mm		290 mm	
	macromodel	micromodel	macromodel	micromodel	macromodel	micromodel
1	10.0	10.0	17.2	21.2	48.1	47.4
2	18.4	18.4	31.5	38.6	85.2	85.4
3	22.2	22.3	38.0	45.9	97.5	96.6
4	29.9	29.9	51.1	61.2	127.6	127.3
5	31.7	31.8	54.4	65.6	138.5	138.7
6	40.8	40.8	69.9	82.3	151.6	151.3
7	42.5	42.5	72.7	85.9	159.6	157.7
8	48.0	47.9	82.1	95.9	164.3	162.0
9	49.8	49.8	85.2	100.3	174.1	174.3
10	59.9	59.9	103.	118.5	188.9	187.4

Relatively amplitude low frequency components of motion which corresponds to oscillation in natural frequencies of the structure are superposed to its response.

4. CONCLUSION

This contribution outlined possible numerical method for solution of masonry separating walls used for partition of underground premises as the explosion prevention. After description of the

experimental gallery and conducted experiment, micromodel, macromodel and the concrete model used in software ANSYS were presented and modal analysis was performed. Nowadays non-linear numerical calculations are often used for complex engineering problems but it should be taken into account that many input data are needed to be discussed.

The lack of specific knowledge of the range of values of shear transfer coefficients brings requirements for more experiments as obtain data could be used for further verification of numerical models. On the other hand, micromodels generated from bricks and mortar joints are already in good agreements with homogenized macromodel which could reduce the time for creating the model and computations.

Separating walls as a way of explosion prevention in underground areas could be designed with the help of advanced numerical procedures on condition that input data and used methods are chosen appropriately.

5. ACKNOWLEDGEMENTS

This paper was financially supported by the project of grant ministry of interior the Czech Republic under the Id. No. VI20152019047, entitled "Development of the rescue destructive bombs for the disposal of statically damaged buildings".

6. REFERENCES

- [1] Makovicka D, Makovicka D, Jr., Dynamic Response of Thin Masonry Wall Under Explosion Effect. In: Jones, N., Brebbia, C.A., Rajedran, A.M.: Structures Under Shock and Impact VII. WIT Press, Southampton, 2002, pp. 47-56.
- [2] Podstawka T, Janovsky B, Horkel J, Vejs L, Pressure Fields Effects Modelling During Explosions of Gases in Closed Buildings on Engineering Structures, Fire Prevention 2001, 1st Part, VŠB-TU, Ostrava, CR, 2001, pp. 333-340.
- [3] CSN EN 1996-1-1: Eurocode 6: Design of masonry structures – Part 1-1: General rules for reinforced and unreinforced masonry structures (in Czech). CEN 2005.
- [4] Makovicka D, Explosion hazard to buildings and design load parameters. In: Jones, N., Brebbia, C.A.: Structures Under Shock and Impact VI. WIT Press, Southampton 2000.
- [5] Mynarzova L, Mynarz M, Study of the effects of transient load on envelope structure Applied Mechanics and Materials, 2014, Vol. 470, pp. 335-339.
- [6] ANSYS® Academic Research, Release 12.1, Help System, ANSYS, Inc.
- [7] Lourenco PB, Computational strategies for masonry structures. Delft University Press, 1996.
- [8] Brozovsky J, Jasek M, Mynarzova L, Maluchova M, Numerical modelling of historical masonry structures, Advanced Materials Research, 2014, Vol. 1020, pp. 182-187.
- [9] Brozovsky J, Kalocova L, Materna A, Constitutive modelling of structural masonry. In Proceedings of VIII. Science conference, technical University of Kosice, 2007. pp. 21 – 25.
- [10] Nguyen CT, Ha HB, Fukagawa R, Two-dimensional numerical modelling of modular-block soil retaining walls collapse using meshfree method, Int. J. of GEOMATE, 2013, Vol. 5, No. 1 (Sl. No. 9), pp. 647-652.
- [11] Brozovsky J, Konecny P, Mynarz M, Sucharda O, Comparison of Alternatives for Remodelling of Laboratory Tests of Concrete, In Proceedings of the Twelfth International Conference on Civil, Structural and Environmental Engineering Computing, 2009, paper 119.
- [12] Kachlakev D, Miller T, Yim S, Chansawat K, Finite Element Modeling of Reinforced Concrete Structures Strengthened with FRP Laminates, Civil and Environmental Engineering, Department California Polytechnic State University, San Luis Obispo, 2001.
- [13] Vaculik J, Unreinforced masonry walls subjected to out-of-plane seismic actions, doctoral thesis, The University of Adelaide, 2012.
- [14] Makovicka D, Kral J, Makovicka D, Jr., Selesovsky P, Brick Masonry Structure Analysis to Gas Explosion on Partition Back Side, Fire Prevention 2002, 1st Part, VSB-TU Ostrava, pp. 221-230.
- [15] Mynarz M, Zdebski J, Mynarzova L, Lepik P, Response of masonry structure to the effects of blast wave induced by deflagration process. In: 5. Magdeburger Brand- und Explosionsschutztag. Magdeburg, 2017.